

## ORIGINAL ARTICLE

# Detailed investigation of ventilation rates and airflow patterns in a northern California residence

Y. Liu<sup>1</sup>  | P. K. Misztal<sup>1</sup>  | J. Xiong<sup>1,2</sup>  | Y. Tian<sup>3</sup>  | C. Arata<sup>4</sup> |  
W. W. Nazaroff<sup>3</sup>  | A. H. Goldstein<sup>1,3</sup> 

<sup>1</sup>Department of Environmental Science, Policy, and Management, University of California, Berkeley, CA, USA

<sup>2</sup>School of Mechanical Engineering, Beijing Institute of Technology, Beijing, China

<sup>3</sup>Department of Civil and Environmental Engineering, University of California, Berkeley, CA, USA

<sup>4</sup>Department of Chemistry, University of California, Berkeley, CA, USA

## Correspondence

Yingjun Liu, Department of Environmental Science, Policy, and Management, University of California, Berkeley, CA, USA.  
Email: yingjun.liu@berkeley.edu

## Funding information

Alfred P. Sloan Foundation, Grant/Award Number: 2015-14166 and 2016-7050

## Abstract

Building ventilation rates and indoor airflow conditions influence occupants' exposure to indoor air pollutants. By making time- and space-resolved measurement of 3 inert tracers steadily released in a single-family house in California for 8 weeks in summer and 5 weeks in winter, this study quantifies the air change rate of the living zone with 2-hour time resolution; estimates airflow rates between the living zone, attic, and crawlspace; and characterizes mixing of air in the split-level living space. Occupant behaviors altered the air change rates, primarily through opening windows and secondarily through operating the heating system. The air change rate correlated with the number of window openings, accounting for 57% of the variability measured across 2 seasons. There were substantial upward interzonal airflows between the crawlspace, living zone, and attic; downward airflows were negligible by comparison. More than 70% of the airflow entering the living zone in the winter and at night during summer came through the crawlspace, rather than directly from outdoors. The airflow from the living zone to the attic increased with the attic-outdoor temperature difference, indicating that buoyancy associated with solar heating of the attic induced airflow from the living zone, increasing the air change rate.

## KEYWORDS

air change rate, interzonal airflow, natural ventilation, occupancy, tracer gas, window opening

## 1 | INTRODUCTION

Ventilation rates and other airflow characteristics in residential buildings strongly influence the concentration levels, dynamic variation, and spatial distribution of indoor air pollutants to which occupants are exposed. Airflows from outdoors into the living zone dilute air pollutants emitted indoors and also introduce outdoor pollutants such as ozone and particulate matter. Airflows into the living zone from coupled spaces, such as the basement, crawlspace, attic, and garage, can introduce air pollutants from those zones. For example, basements and crawlspaces can be important pathways for the intrusion into the living zones of radon and volatile organic compounds (VOCs) released from soil and groundwater.<sup>1-3</sup> Internal airflows within living zones, from room to room and from floor to floor, affect

spatial variation of indoor air pollutants.<sup>4</sup> A good understanding of building airflows and their underlying mechanisms are a key to accurate prediction of indoor pollutant exposure in residences.

Air change rate ( $A$ ), the total rate of outdoor air entering a building or an indoor space divided by its volume, is a commonly used metric to characterize building ventilation.<sup>5</sup> For a residence experiencing air change by natural ventilation plus infiltration, outdoor air can enter the living space through intentional openings (such as open windows), through unintentional leaks in the building envelope, and via coupled spaces (such as crawlspaces, basements, and attics). Air change rates have been measured in a large number of homes in the United States and Europe using tracer gas techniques.<sup>6</sup> In most cases, these have been one-time measurements sampled over periods of a day to a week or longer.<sup>5</sup> Time-resolved measurements

of air change rate in individual buildings monitored over extended periods are uncommon, yet such data can provide important clues about key factors affecting air change rates. Earlier time-resolved measurements were used to evaluate relationships between infiltration rates and meteorological conditions, primarily wind speed and indoor-outdoor temperature difference.<sup>7</sup> More recently, long-term observations have suggested that the behavior of occupants, in particular in their use of windows, can influence air change rates of occupied residences, often more strongly than the variable meteorological conditions.<sup>8-10</sup> For example, in a year-long observational study in an occupied townhouse in the United States, Wallace et al<sup>9</sup> found that the mean air change rate (measured with 100-minute resolution) increased from 0.44 h<sup>-1</sup> for window-closed conditions to 1.57 h<sup>-1</sup> with some windows open or the attic fan on. In monitoring air change rates in 5 residences in Denmark across 4 seasons, Bekö et al<sup>10</sup> suggested that the observed variation by season and by occupancy was largely associated with differences in window-opening behavior. One limitation of these 2 studies is that the record of window-opening behavior is limited, that is, solely relying on occupants' recollection. This limitation prevents more thorough quantitative investigation of the relationship between air change rate and window openings.

Building interzonal airflows have been studied utilizing multiple tracers.<sup>11,12</sup> Earlier studies of the residential interzonal airflows were often carried out in research houses.<sup>1,13-19</sup> Field measurements in dwellings under normal occupancy conditions are limited,<sup>4,10,20-22</sup> and continuous measurements investigating diel patterns or seasonal variation are rare.<sup>4</sup> Available measurements in occupied dwellings generally show considerable airflow rates to the living zones from the studied coupled spaces, including garages,<sup>21,22</sup> basements,<sup>20,22</sup> or common apartment hallways.<sup>22</sup> For example, a study of 35 residences in Boston found that, on average, 26% of air entering the living zone came from the basement in summer and 47% in winter.<sup>22</sup> Mixing of air within the living zone has been observed to vary among residences.<sup>4,10</sup> A study of 126 US houses found that children's bedrooms received an average of 55% ( $\pm 18\%$ ) of air from elsewhere in the residence.<sup>4</sup>

We report here on a detailed investigation of air change rates and interzonal flows in a single-family house in northern California. We quantify temporal variability under normal occupancy conditions and explore factors that affect the variability. This study is part of an intensive observational campaign to understand the exposure and sources of indoor VOCs and bioaerosols. To investigate air change rates and interzonal flows, 3 deuterated inert tracer gases were injected at constant rates into 3 zones of the house and measured continuously at multiple locations using a proton-transfer-reaction time-of-flight mass spectrometer (PTR-TOF-MS). Extensive metadata were acquired to characterize time-resolved environmental and operational conditions of the household. The study results presented in this report are organized into 3 main topics. (i) Continuous air change rate of the living zone is assessed with 2-hour resolution. Factors that drive air change rate, in particular occupants' behaviors, are explored. (ii) Airflow rates among the crawlspace, living zone,

## Practical Implications

The results contribute to a better understanding of airflow characteristics in the residential environment, which has foundational importance for accurate prediction of indoor pollutant exposure. The results illustrate how occupants, via window-opening and heating system operation behaviors, substantially influence household air change rate. The observed airflow patterns and quantitative tracer measurement results illuminate the important point that air contaminants can intrude into occupied spaces from coupled zones such as the crawlspace.

and attic are evaluated. Their diel and seasonal variations, as well as the underlying driving factors, are discussed. (iii) Air mixing in the split-level living zone is characterized. Uncertainties in applying tracer methods to non-well-mixed conditions are explored utilizing an extensive empirical data set for this house.

## 2 | METHODS

### 2.1 | Observational campaign

Extensive observational monitoring during 2 seasons was conducted in a single-family house in Oakland, California. The first observational period (summer campaign) was 8 weeks in duration from mid-August to early October, 2016. The second period (winter campaign) spanned 5 weeks from late January to early March, 2017. Oakland has a Mediterranean climate, with dry, sunny, and warm summers, contrasting the wet and cool winters. The median noontime outdoor air temperature was 20 and 12°C during the summer and winter campaigns, respectively.

The studied house, built in the 1930s of wood-frame construction, has a split-level living zone, an unoccupied attic above, and a small basement and larger crawlspace below. The internal volume of the living zone is estimated from direct measurements to be 350 m<sup>3</sup> (after subtracting the volume of major cabinets, closets, and furniture). As shown in Figure S1, there are 3 bedrooms and 2 bathrooms on the upper level (~150 m<sup>3</sup> in total volume) and a kitchen, family room, and living room on the lower level (~200 m<sup>3</sup> in volume). Two adult occupants (age within the range 55-65 years) live in the house. In addition to normal house operation conditions (occupied periods), the occupants were deliberately away from the house for a few days at the beginning of the winter campaign and for a week at the end of the summer campaign; during these vacant periods, the house windows and doors were all closed.

The house is equipped with central heating, but no air conditioning. A decades-old natural gas-fired gravity furnace (buoyancy-driven, with no central fan) is situated in the crawlspace with heating system ducts conveying air to each room in the living zone and a

large return duct extracting air from the foyer. The furnace ran intermittently during the winter campaign and was off during the summer campaign. During winter, a programmable thermostat was set to provide heat to 18°C for 1.5 hours each morning and for 4.5 hours each evening; at other times, a sufficiently low set point meant that the heat was effectively off. Overall, the heating system operated 8% of the time during the winter campaign. The house has no mechanical ventilation other than exhaust fans above the stove (on for <0.5% of the time during monitoring) and in the bathrooms (on for ~2% of the time). Interior doors connecting rooms in the living zone were normally kept open, including at night. The entrances from the living zone to the substructure (basement and crawlspace) and to the attic were generally closed. The basement room contained a washing machine, clothes dryer (with exhaust ducted outdoors), and storage space, which was occasionally accessed. The exterior walls of the house are uninsulated; the attic floor is covered with fiberglass batts. There are penetrations from the living space into the cavities of interior and exterior walls associated with plumbing pipes, electric wiring, and heating system ductwork.

Temporally and spatially resolved measurements of gases including VOCs and inert tracers were made using a PTR-TOF-MS (Ionicon Analytik GmbH, Austria, PTRTOF 8000). Ozone and carbon dioxide (CO<sub>2</sub>) were measured simultaneously using an ozone monitor (Thermo Scientific, 49i) and a CO<sub>2</sub> monitor (LI-COR, LI-820), respectively. In addition, size-resolved bioaerosol particles were measured using an ultraviolet aerodynamic particle sizer (TSI, 3314), as reported elsewhere.<sup>23</sup>

The gas-analysis instruments were situated in a detached garage about 5 m from the house. Air was continuously drawn through separate 30-meter-long 6.4-mm (¼" OD) PFA sampling tubes at a constant flow rate of ~2 L/min from 6 locations: outdoors, kitchen (representing the lower living zone), landing at the top of the half flight of stairs (with doors open to the bedrooms, representing the upper living zone), crawlspace, basement, and attic. (See Figure S1). A 2.0-µm pore size PTFE particle filter was installed on the intake end of each sampling line. The gas instruments regularly and automatically switched between subsampling from these lines through a 6-way manifold (NResearch, 648T091; PTFE inner contact surfaces). The total inflow rates of the 3 gas-sampling instruments were ~1.4 L/min. Two different sampling sequences were employed during observational monitoring. During some periods, data were collected with spatial resolution emphasized, switching regularly through each of the 6 inlets at 5-minute intervals (ie 30 minutes for a full cycle). Other sampling periods were designed to collect data with higher temporal resolution in the living zone; in this case, the 30-minute cycle involved only 3 locations: outdoors (5 minutes), kitchen (20 minutes), and bedroom areas (5 minutes).

Extensive metadata were acquired to characterize general environmental and operational conditions in the household. More than 50 wireless sensors were used to monitor time-resolved room occupancy (motion), appliance use (on/off), door/window open status (open/closed), and indoor temperature and humidity. Data from the temperature/humidity sensors (Netatmo, France)

were reported every 5 minutes. The other sensors (SmartThings) responded to changes of status/values (with time resolution of less than 1 second). Occupants also maintained daily presence/absence and activity logs to complement the automatically acquired metadata. Outdoor temperature, humidity, and rainfall were obtained from a weather station located 3.5 km north of the house, while wind direction and wind speed were obtained from a weather station 10 km south, all reporting time-average values with hourly resolution.

Metadata relevant in this analysis are summarized below. In total, open status of 7 windows and 2 doors was monitored in situ by wireless sensors; the (rare) use of other windows was manually recorded by occupants. The number of open doors and windows ( $N_{op}$ ) was calculated for continuous 2-hour periods by summing up the fraction of open time for all the windows and doors, resulting in better than single integer resolution. Furnace operation and dryer use were monitored by register temperature and dryer vibration, respectively. Use of extraction fans in the bathrooms was indirectly indicated by relative humidity in the bathrooms (shower time). Use of extraction fan above the stove was recorded by the occupants. Figure S2 displays the median and interquartile ranges of diel temperature variation in the 6 spaces where the measurements were made in the summer and winter campaigns. Figure S3 shows average wind direction and speed observed during the summer and winter campaigns. For calculating the temperature difference between the indoor (living zone) and outdoor air ( $T_{in} - T_{out}$ ),  $T_{in}$  was taken as the average of air temperature measured in the kitchen and bedroom area.

## 2.2 | Tracer methods

Three deuterated alkenes measurable by PTR-TOF-MS were selected as inert tracers to study air change rates and interzonal flow rates. The 3 gases were propene-d6 (C<sub>3</sub>D<sub>6</sub>), propene-d3 (CD<sub>3</sub>CH=CH<sub>2</sub>), and butene-d3 (CD<sub>3</sub>CH<sub>2</sub>CH=CH<sub>2</sub>). They were chosen based on their low toxicity to human occupants, low tendency to sorb to interior surfaces (ie they possess high vapor pressures and low octanol-air partition coefficients), negligible background levels in indoor air, and unique exact masses allowing for unambiguous identification and quantification by PTR-TOF-MS (see Supporting Information).

Propene and butene can react with O<sub>3</sub> and OH; the estimated loss rates of these compounds in reacting with oxidants indoors are <0.03 h<sup>-1</sup>,<sup>24</sup> assuming that the respective concentrations are bound by  $C_{OH} < 2 \times 10^5 \text{ cm}^{-3}$  and  $C_{O_3} < 10 \text{ ppb}$ . This reactivity loss rate is an order of magnitude lower than typical air change rates measured indoors. The small effect of chemical loss of the selected alkene tracers was confirmed experimentally, by comparing the decay rates of the selected tracers together with that of a non-reactive tracer, difluoroethane, in the living zone following pulsed injections during normal house operating conditions.

Propene-d3 (98%) and butene-d3 (98%) were obtained from Cambridge Isotope Laboratories, Inc., and propene-d6 (99%) from Isotec, Inc. Pressurized aluminum cylinders (see Supporting Information) were prepared for each alkene tracer at 400-600 ppm

in nitrogen. The cylinders were placed in the detached garage and tracers were continuously released at a controlled flow rate (5–15 cm<sup>3</sup>/min) via 3.2-mm (1/8" OD) PFA tubing into different locations in the house. The outlet of the tubing was attached to a small fan continuously operated to promote initial mixing with indoor air.

Two tracer deployment schemes were used during each campaign. During some periods, the tracers were deployed to study interzonal airflows between the living and unoccupied house zones. In this case, propene-d6 was released in the attic, butene-d3 in the living zone, and propene-d3 in the crawlspace. During other periods, the tracers were deployed to emphasize studying air change rates and mixing in the living zone, with butene-d3 released in the upper (summer)/lower (winter) living zone, propene-d6 in the lower (summer)/upper (winter) living zone, and propene-d3 in the crawlspace.

The response of PTR-TOF-MS to the individual tracers was calibrated at the end of each campaign using dilutions derived from the custom-made gas cylinders. Detailed calibration results are presented in the Supporting Information (Figure S4). The uncertainty for the tracer measurement is less than 5%. The small uncertainty is due to that calibration and tracer release used the same cylinders and that measured levels were several orders of magnitude above detection limits. Figures S5 and S6 present time series of tracer mixing ratios measured in the 6 spaces of the studied house, for summer and winter campaigns, respectively.

### 2.3 | Calculation of air change rate in the living zone

Air change rates were determined by approximating the occupied internal volume of the house as a single zone. As presented later in Section 3.2, crawlspace and attic generally served as one-way paths for air exchange between the living zone and outdoors, supporting the single-zone approximation. Under this approximation, the mass balance of a tracer released in the living zone is given by:

$$\frac{dC_{in}(t)}{dt}V = E - A(t) \cdot C_{in}(t) \cdot V \quad (1)$$

where  $C_{in}(t)$  is the averaged tracer concentration in the living zone (ppb; part per billion by volume);  $V$  is the volume of the living zone (m<sup>3</sup>);  $E$  is the emission rate of the tracer in the living zone (mm<sup>3</sup>·h<sup>-1</sup>). Assuming air change rate,  $A(t)$ , is constant over an integration time period,  $\Delta t$ , then  $A(t)$  can be evaluated by integrating Equation (1):

$$A(t) = \frac{E\Delta t - (C_{in}(t+\Delta t) - C_{in}(t))V}{C_{in}(t)V\Delta t} \quad (2)$$

In application,  $E$  is experimentally controlled (known),  $V$  is the measured value (350 m<sup>3</sup>), and  $\Delta t$  is 2 hours. The indoor concentration,  $C_{in}(t)$ , is approximated as the weighted mean of tracer concentrations measured in the kitchen and bedroom area (see further detail in Supporting Information).

Sources of uncertainty in calculating air change rates using Equation (2) include the approximation of a properly time- and space-averaged indoor tracer concentration. As a check on the accuracy of the approach, an additional experiment in the living zone showed that air change rates determined from steady injections agreed well with those determined from the tracer decay method (Figure S7). Another consistency check is comparing air change rates estimated using tracers released in the upper and lower living zones, respectively, during the living zone-focused tracer deployment periods. Figure S8 compares the 2 estimates of air change rates, demonstrating good agreement for both winter and summer campaigns, in particular for the lower range of air change rate. In the following analysis, the geometric mean of air change rate calculated for each 2-hour period is taken as the best estimate.

To discuss how the assumption of well-mixed volumes affects estimates of air change rates (cf. Section 3.3), the time-resolved air change rate was also calculated based on single-point measurements of a single tracer. That is, for use of Equation (2),  $C_{in}(t)$  was taken as the tracer concentration measured either in the kitchen or in the bedroom area. For living zone-focused tracer deployment periods, 4 alternative sets of air change rates were obtained, corresponding to measurements of upper/lower living zone tracer in the kitchen/bedroom area.

### 2.4 | Evaluation of multizone airflow rates

Interzonal airflow rates among the living zone, crawlspace, and attic are evaluated from tracer measurements using a multizone mass balance approach.<sup>25–28</sup> During tracer deployment periods that focused on interzonal airflows, a distinct tracer  $i$  was released in each of the 3 spaces  $i$  ( $i = 1, 2, 3$ ). The tracer concentrations in outdoor air (space 0) were negligible (Figures S5 and S6). At steady state, the mass balances of the 3 tracers in the 3 indoor spaces are given in matrix form by:

$$\mathbf{E} = \mathbf{C}\mathbf{Q} \quad (3)$$

$$\begin{pmatrix} E_{11} & 0 & 0 \\ 0 & E_{22} & 0 \\ 0 & 0 & E_{33} \end{pmatrix} = \begin{pmatrix} c_{11} & c_{12} & c_{13} \\ c_{21} & c_{22} & c_{23} \\ c_{31} & c_{32} & c_{33} \end{pmatrix} \begin{pmatrix} \sum_{j=0}^3 q_{1j} & -q_{12} & -q_{13} \\ -q_{21} & \sum_{j=0}^3 q_{2j} & -q_{23} \\ -q_{31} & -q_{32} & \sum_{j=0}^3 q_{3j} \end{pmatrix}$$

where  $\mathbf{E}$  is a diagonal emission matrix, with entries  $E_{ij}$  representing emission rate of tracer  $i$  in indoor space  $i$ , in mm<sup>3</sup>·h<sup>-1</sup>;  $\mathbf{C}$  is a 3 × 3 concentration matrix, with entries  $c_{ij}$  representing concentration of tracer  $i$  in indoor space  $j$ , in ppb;  $\mathbf{Q}$  is a 3 × 3 flowrate matrix, in m<sup>3</sup>·h<sup>-1</sup>. For matrix  $\mathbf{Q}$ , the off-diagonal entries  $q_{ij}$  represent the airflow rates from indoor space  $i$  to indoor space  $j$ ; and the diagonal entries  $\sum_{j=0}^3 q_{ij}$  represent the sum of airflow rates leaving space  $i$ . The sum of the entries in row  $i$  of matrix  $\mathbf{Q}$  is airflow rate  $q_{i0}$  from space  $i$  to outdoors. Based on mass balance for air, the sum of the entries in column  $i$  of matrix  $\mathbf{Q}$  is airflow rate  $q_{0i}$  from outdoors to space  $i$ .

Based on Equation (3), for a non-singular concentration matrix  $C$ , we can derive the flow matrix  $Q$

$$Q = C^{-1}E \quad (4)$$

Characteristic flow matrixes  $Q$  were estimated using Equation (4) for night (3:00-7:00) and afternoon periods (16:00-20:00), respectively, in each campaign. In applying Equation (4),  $E$  is experimentally known. The concentration matrix  $C$  was assessed by means of taking hourly median tracer concentrations across the monitored days for each tracer in each space, and then averaging over the selected 4-hour periods. For the living zone, hourly median concentrations of tracer  $i$  were taken as the average of hourly median concentrations measured in the kitchen and bedroom areas, weighted by the respective volumes of the lower and upper living zones. For the attic and crawl space, the calculation was based on single-point measurements in each space. The resultant concentration matrix  $C$  preserved the general features of flow patterns in the house, but attenuated high-frequency variations, which were partly associated with the time-varying state of mixing. In addition, the specific 4-hour periods (3:00-7:00 and 16:00-20:00) were chosen based on times when hourly median tracer concentrations were relatively stable, so that the steady state assumption inherent in Equation (4) was approximately satisfied.

### 3 | RESULTS AND DISCUSSION

#### 3.1 | Air change rate in the living zone

##### 3.1.1 | Characterizing the air change rate

In this section, the air change rate measured in the living zone is characterized in several ways, exploring seasonal variation, diel variation, and the variation attributable to occupant behaviors. Figure 1 presents the cumulative distributions of air change rate in the living zone as determined with 2-hour resolution during the occupied and vacant periods in the summer and winter campaigns, respectively. Consistent with long-term observations of air change rates previously reported,<sup>9,29</sup> the data sets can be approximated by lognormal distributions. The highest variability in air change rate was observed during the summer occupied period, with the 5th and 95th percentiles differing by a factor of 4. The air change rates met corresponding ventilation requirements ( $\geq 0.29 \text{ h}^{-1}$  according to ASHRAE Standard 62.2) for 88% of the time in the summer occupied period, and for 65% of the time in the winter occupied period.<sup>30</sup>

Occupancy clearly has a strong influence on the measured air change rates. The air change rates in the summer occupied period ( $GM = 0.47 \text{ h}^{-1}$ ;  $GSD = 1.6$ ) and winter occupied period ( $GM = 0.33 \text{ h}^{-1}$ ;  $GSD = 1.3$ ) were consistently higher than the vacant periods in both seasons ( $GM = 0.25$  and  $0.22 \text{ h}^{-1}$ ;  $GSD = 1.2$ ). Indeed, the 90th percentile of air change rates during the vacant period corresponded to only the 15th percentile in the occupied period in summer and the 25th percentile in winter.

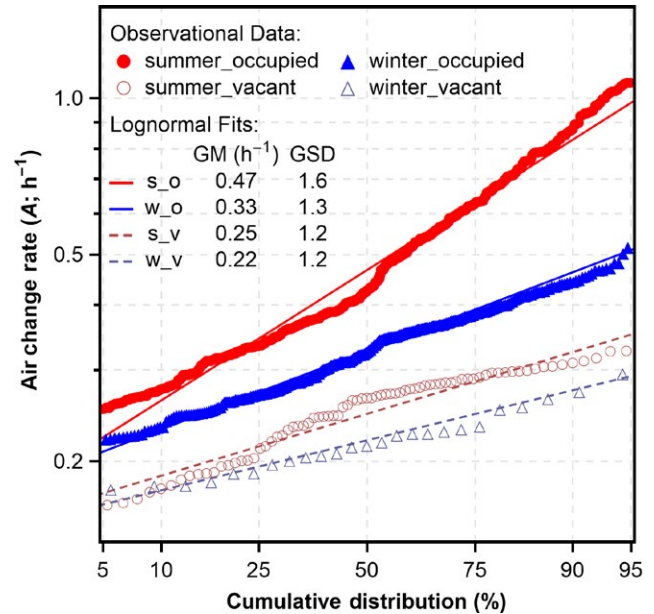


**FIGURE 1** Cumulative distributions of air change rates ( $A$ ) measured with 2-hour resolution. Data are presented for summer occupied periods ( $s_o$ ; red filled circle;  $n = 486$ ), summer vacant periods ( $s_v$ ; red open circle;  $n = 85$ ), winter occupied periods ( $w_o$ ; blue filled triangle;  $n = 317$ ), and winter vacant periods ( $w_v$ ; blue open triangle;  $n = 27$ ). The solid and dashed lines represent fits of lognormal distributions for occupied and vacant periods, respectively, for each season. The geometric mean ( $GM, \text{h}^{-1}$ ) and geometric standard deviation ( $GSD$ ) of each fitted distribution is listed

Another feature evident in Figure 1 is seasonal variation. For occupied periods, the air change rate in the summer covered a wider dynamic range with more frequent elevated values compared with winter. Specifically, the 5th percentile values were similar, but the 95th percentile differed by a factor of 2. Other studies in residences have also reported higher air change rates in summer than in winter.<sup>9,10</sup>

Figure 2A displays the diel variation of air change rates in the summer (left) and winter (right) campaigns. For the summer occupied period, strong diel variation was observed. The median value of air change rates was consistently about  $0.3 \text{ h}^{-1}$  overnight (22:00-6:00), then increased slowly during the day, peaking at  $0.7 \text{ h}^{-1}$  in the evening, and then quickly declined. By comparison, in the winter occupied period, and in the vacant periods for both seasons, the air change rates were smaller and no prominent diel variation was observed. Stronger diel variation in summer was reported by Bekö et al in their study of 5 residences across 4 seasons.<sup>10</sup>

##### 3.1.2 | Factors influencing the air change rate

Figures 2B-D present diel variation of 3 factors that are expected to influence the air change rates, including the number ( $N_{op}$ ) of open windows and doors, the temperature difference ( $T_{in} - T_{out}$ ) between

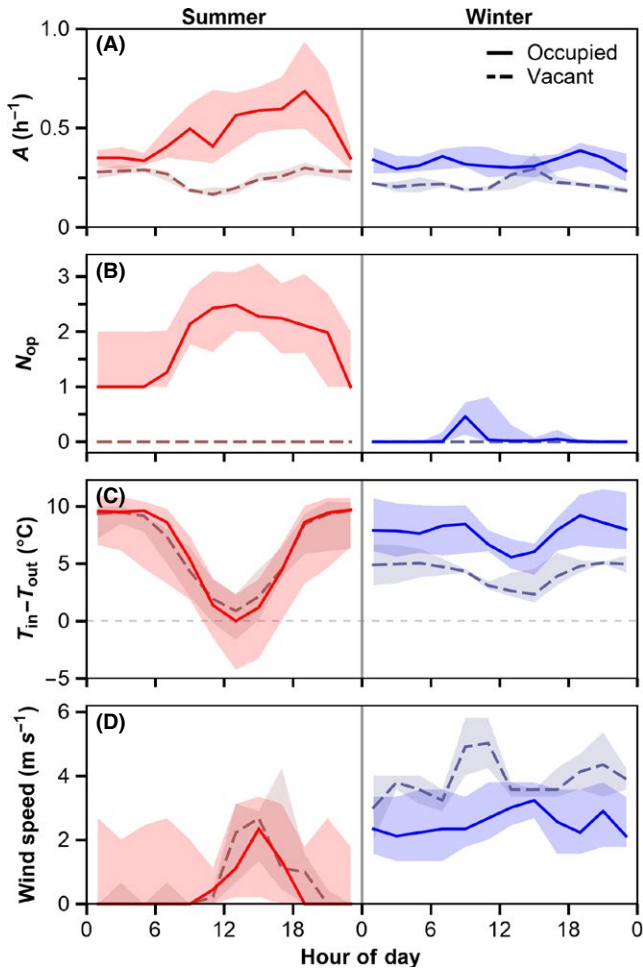


**FIGURE 2** Diel variation of (A) air change rate, (B) number ( $N_{op}$ ) of opened windows and doors, (C) temperature difference ( $T_{in}-T_{out}$ ) of indoor and outdoor air, and (D) outdoor wind speed. Data are shown for occupied and vacant periods, (left) in summer in red and red-gray, respectively, and (right) in winter in blue and blue-gray, respectively. Solid and dashed lines, respectively, represent medians of occupied and vacant periods. The shaded regions represent the interquartile ranges. The data sets are shown in 2-hour resolution.

indoor and outdoor air, and outdoor wind speed, respectively. Increases of each of these 3 parameters are expected to enhance air change rates.<sup>5</sup> An important issue to resolve in this section is the relative and specific influence of these 3 parameters.

Comparing Figure 2B–D to A, it is evident that the pattern of house opening condition associates well with the observed diel variation of air change rates. In the summer occupied period (Figure 2B left), 1 window was typically open from 10:00 PM to 6:00 AM, whereas 2 or more windows were often open starting from 8:00 AM until 10:00 PM. The night period with 1 window open corresponded to when the low median values of air change rates ( $\sim 0.3 \text{ h}^{-1}$ ) were observed. All windows and doors in the house were closed in the vacant periods in both seasons and for most of the time during the winter occupied period. Correspondingly, the median values of air change rates for these 3 periods were smaller

than during the summer occupied period and exhibited little diel variation.

Temperature difference is a second important factor influencing air change rates. The occupants sporadically used the furnace to heat the house in the winter. Along with occupant metabolism and other energy-transforming activities (such as cooking), the effect was a higher median indoor temperature in the occupied winter period than in the vacant winter period (data not shown), and hence a larger indoor-outdoor temperature difference throughout entire days (Figure 2C, right). Correspondingly, higher air change rates were observed for the occupied winter period (Figure 2A, right). In the summer, primarily driven by the diel swing of outdoor temperature,  $T_{in}-T_{out}$  declined from  $9^\circ\text{C}$  before sunrise to near zero at noon, then increased slowly back to  $9^\circ\text{C}$  in the evening (Figure 3C, left), for both vacant and occupied periods. As the median temperature difference increased in the evening, the median air change rate during occupied periods increased from  $0.4 \text{ h}^{-1}$  near noon to  $0.7 \text{ h}^{-1}$  (Figure 2A, left), whereas median number of windows and doors open stayed nearly constant at  $\sim 2$  (Figure 2B, left). The median air change rate in the vacant period also showed a small but clear dip when the temperature difference was smaller.

The influence of wind speed on measured air change rates is less clear in Figure 2. In the summer, it was common for the study site to experience a weak westerly sea breeze (Figure S3). Median wind speeds were close to zero starting from the evening until mid-morning, then peaked at  $2 \text{ m}\cdot\text{s}^{-1}$  in mid-afternoon owing to diurnal land heating (Figure 2D, left). In the winter, stronger southerly or northerly winds were associated with Pacific winter storm systems (Figure S3). Median wind speeds were commonly above  $2 \text{ m}\cdot\text{s}^{-1}$  during entire days (Figure 2D, right). These variations were, however, not directly reflected in the seasonal and diel variation of air change rates displayed in Figure 2A.

The importance of the 3 factors is further examined via correlation plots. Figure 3A displays logarithmically transformed air change rates (with 2-hour resolution) plotted against number of open windows and doors for all measured data. A good correlation is observed (Pearson's correlation coefficient  $r = .75$ ). A linear fit of the two alone can explain 57% of the variance in logarithmically transformed air change rates. This result reinforces the point that the number of window (and door) openings is a key factor influencing the air change rates in the studied house.

Figure 3B displays the 2-hour air change rates plotted against the absolute indoor-outdoor temperature difference for a subset of data when the house was almost completely closed ( $N_{op} < 0.05$ ), that is, when infiltration would have clearly dominated. The presented data are colored according to wind speed,  $u$  (green for  $u < 2 \text{ m}\cdot\text{s}^{-1}$  and orange for  $u \geq 2 \text{ m}\cdot\text{s}^{-1}$ ). There is a clear increasing trend of air change rate with increasing  $|T_{in}-T_{out}|$  for conditions at lower wind speed (Pearson's  $r = .69$ ). The magnitude of the temperature effect with windows closed is about  $0.13 \text{ h}^{-1}$  per  $10^\circ\text{C}$ , comparable to values reported for other houses.<sup>9,29,31,32</sup> The relationship is more variable at higher wind speeds, suggesting that wind also influences air change rate, although to a smaller extent than temperature difference at this

house. The effects of temperature difference and wind speed are less clear with house windows open (cf. Figure S9).

Regression of air change rate on a combination of  $N_{op}$ ,  $|T_{in}-T_{out}|$ , and  $u$  is performed using 3 approaches: a mechanistic model and 2 adjusted models. The mechanistic model is an extension of the Lawrence Berkeley Lab infiltration model (LBLX) to include natural ventilation.<sup>33</sup> The 2 adjusted models use modified representations of natural ventilation. Details of the 3 models and regression results are included in the Supporting Information (see Figure S10 and Table S1). As a highlight of the regression result, an adjusted model factoring the stack effect of the attic ( $T_{attic}-T_{out}$ ) into natural ventilation achieved a better fit to observations than the default LBLX model. This result provides additional support for the inference that the sun-heated attic constituted a meaningful driving force for ventilation in the living zone (see Section 3.2).

The results in this section highlight the importance of the occupants' influence on air change rates by opening windows and doors. A single simplified parameter of house open conditions, that is, the number of window and door openings, can explain the marked diel trend of air change rates in the summer as well as 57% of variance in the full data set. Although not explored here, other detailed house opening parameters, such as the size and position of openings, might make additional contributions to the observed air change rates. Previous studies have suggested that the window-opening behavior of occupants influenced air change rates in occupied residences,<sup>9,10</sup> but quantitative characterization was limited to the effect of opening 1 window.<sup>34</sup> The results reported here are the first quantitative evaluation over time of periodically opening multiple windows and doors in occupied residences during normal occupancy. Although limited to 1 house, the results provide some new quantitative insight regarding human occupant influences on air change rates in a residence.

Another aspect of occupant behavior influencing air change rates is through regulating the temperature of indoor air. The use of the furnace in the winter led to larger indoor-outdoor temperature differences in the occupied period than during the vacant period, which in turn led to consistently higher air change rates for the occupied period (Figure 2A). An analogous effect could be anticipated for air-conditioned houses in warm summer climates. By cooling the residence using an air conditioner, the absolute indoor-outdoor temperature difference is increased, enhancing air change rates. To summarize, the adjustment of room temperature in heating or cooling seasons by occupants, to maintain a thermally comfortable indoor environment, can indirectly lead to higher values of air change rates through amplifying the stack effect. Specific heating and cooling operation decisions, including hours of use and temperature set point(s) could, therefore, influence residential air change rates.

### 3.2 | Airflow pattern in the house

Airflows among 3 major compartments of the house—the attic, living zone, and crawlspace—were studied by continuously releasing a different tracer into each of the 3 spaces for extended periods

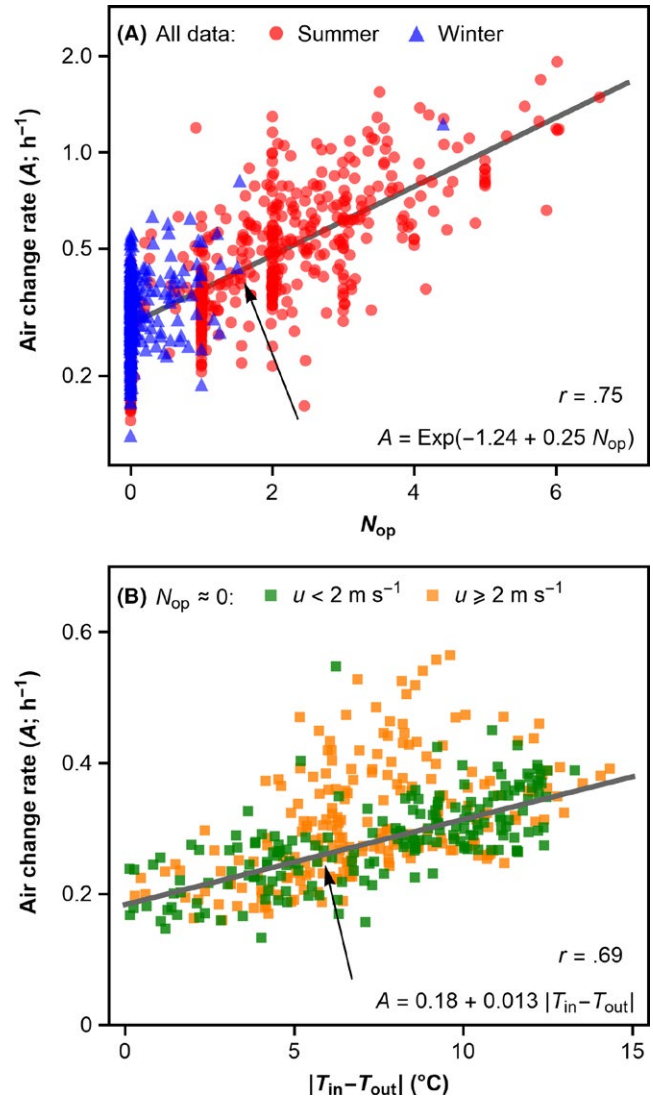


**FIGURE 3** Scatter plot of air change rate against (A) number of opened windows and doors ( $N_{op}$ ) and (B) absolute temperature difference of indoor and outdoor air  $|T_{in}-T_{out}|$ . Panel (A) presents all the data, colored in red and blue for summer and winter, respectively. The line represents a linear fit of the logarithm of air change rate vs  $N_{op}$ . Panel (B) presents a subset of data when the house was closed ( $N_{op} < 0.05$ ). Data are colored by wind speed ( $u$ ): in orange ( $u \geq 2.0 \text{ m}\cdot\text{s}^{-1}$ ) and green ( $u < 2.0 \text{ m}\cdot\text{s}^{-1}$ ). The line represents a linear fit of air change rate vs  $|T_{in}-T_{out}|$  for  $u < 2.0 \text{ m}\cdot\text{s}^{-1}$

of the observational campaigns. Figure 4 shows hourly variations of the mixing ratios of the 3 tracers during occupied periods in the summer and winter. An essential feature revealed in Figure 4 is that tracers were rarely detected in the indoor spaces below their injection level. For the tracer injected into the attic, the median mixing ratio ranged from 0.8 to 2.6 ppb in the attic (Figure 4A). The median values of the attic-injected tracer were, however, below the detection limit (0.02 ppb) for the other spaces in the summer and just above the detection limit for the kitchen and bedroom areas in the winter. Similarly, for more than 70% of the time, the tracer injected into the living zone was not detected (<0.006 ppb) in the

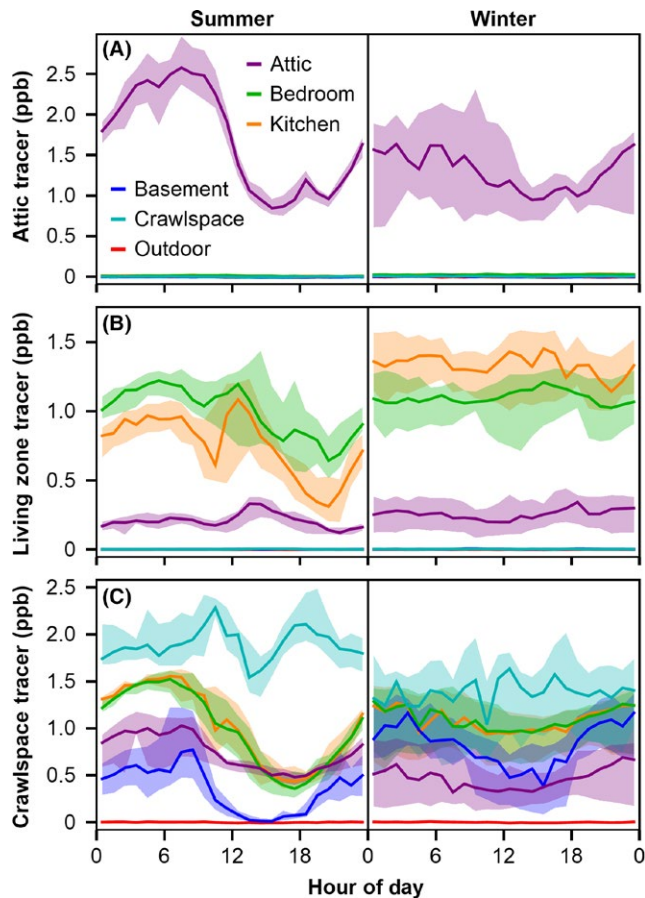


**FIGURE 4** Hourly variation of mixing ratios of tracer compounds injected into (A) attic, (B) living zone, and (C) crawlspace. Data are shown for the occupied periods in summer (left) and winter (right) campaigns. Data are colored in purple, green, orange, blue, cyan, and red colors for mixing ratios measured in the attic, bedroom area, kitchen, basement, crawlspace, and outdoors, respectively. The solid line and shaded regions, respectively, represent the median and interquartile ranges of mixing ratios for each hour of the day. The summer data correspond to periods 1, 3, 5, and 7 in Figure S6 and the winter data correspond to period 3 in Figure S7. The presented mixing ratios are normalized by injection rates (varied between campaigns), so that the summer and winter data are directly comparable for each tracer compound

subfloor spaces (crawlspace and basement) (Figure 4B). In contrast, the tracer injected into the crawlspace was consistently observed in all the above-floor indoor spaces, and the tracer injected into the living zone was consistently observed in the attic. Clearly, air routinely infiltrated upward through the house, across the boundaries separating the living space from the unoccupied coupled spaces, but rarely flowed downward (Figure 4C). Figure 4 also shows that the concentrations of all 3 tracers differed considerably between the summer and winter. Diel variation was observed for some tracers in the summer. The airflow patterns among the attic, living zone, and crawlspace changed by season and by hour of day.

Hourly medians of tracer concentrations presented in Figure 4 were used to estimate volumetric airflow rates among the attic,

living zone, and crawlspace, as described in Section 2.4. Figure 5 presents the determined airflow rates at night (3:00-7:00) and in late afternoon (16:00-20:00) in the summer and winter, respectively, to display both seasonal and diel variation. The next paragraphs summarize major features of airflows into and out of each of the 3 spaces and discuss the driving factors.

The airflow entering the crawlspace mainly came from outdoors. The total inflow rates showed small diel variation, likely attributable to the diel variation of temperature differences between the crawlspace and outdoors (Figure S11). Seasonal variation was larger: Total airflow rate into the crawlspace was about 40% higher in winter than in summer, both at night and during the afternoon. The seasonal difference was driven primarily by wind, modulated by the crawlspace-outdoor air temperature difference. In addition, as the house is located in a residential neighborhood with its front and most exposed face oriented to the south (cf. Figure S1), the westerly summer sea breeze could have a weaker impact on flows through the building envelope than the common southerly or northerly wind in the winter (Figure S3). The net effect is that airflow rates into the crawlspace were lower in the summer than in the winter for both day and night.

For the attic, about half of the entering airflow came from outdoors and the other half came from inside the house, both from the living zone and from the crawlspace. The tracer gas results indicate a direct airflow path connecting the crawlspace to the attic. Such flow was previously reported in a research house in Illinois,<sup>15</sup> and it may occur through the wall cavities of this wood-framed house. Strong diel variation was observed for the airflows into the attic. The total airflow rate in the afternoon was 2.5 times higher than the nighttime flow rate in the summer, and, in the winter, it was 1.5 times higher.

There is evidence that heating of the attic and the associated stack effect may have influenced the air change of the living zone by means of inducing enhanced flow from the living zone into the attic. Note that the median attic-outdoor temperature difference was less than 5°C at night. However, with heating of the roof by the sun, the afternoon attic temperature increased above the outdoor value by about 15°C during the summer and 10°C in the winter (Figure S11). The larger temperature difference is associated with higher flow rates into the attic from the living zone in the afternoon. Specifically, the estimated airflow rate from the living zone to the attic was 115 m<sup>3</sup>·h<sup>-1</sup> during summer afternoons and 75 m<sup>3</sup>·h<sup>-1</sup> during winter afternoons, as compared to 28 and 46 m<sup>3</sup>·h<sup>-1</sup> for summer and winter nights, respectively. One feature of the summer afternoons is that more windows were open in the living zone, which would have lowered the resistance for the heated attic to draw air upward from the living zone.

Wind also influences flows into the attic. The airflow rate from outdoors into the attic at night in the windier winter was twice that of the calmer summer (Figure 5A,C), even though the attic-outdoor temperature difference was comparable at night in the 2 seasons. For afternoon periods, even though temperature differences were higher in summer, the flow rates from outdoors into the attic were higher in the winter, most likely because of the stronger winds.



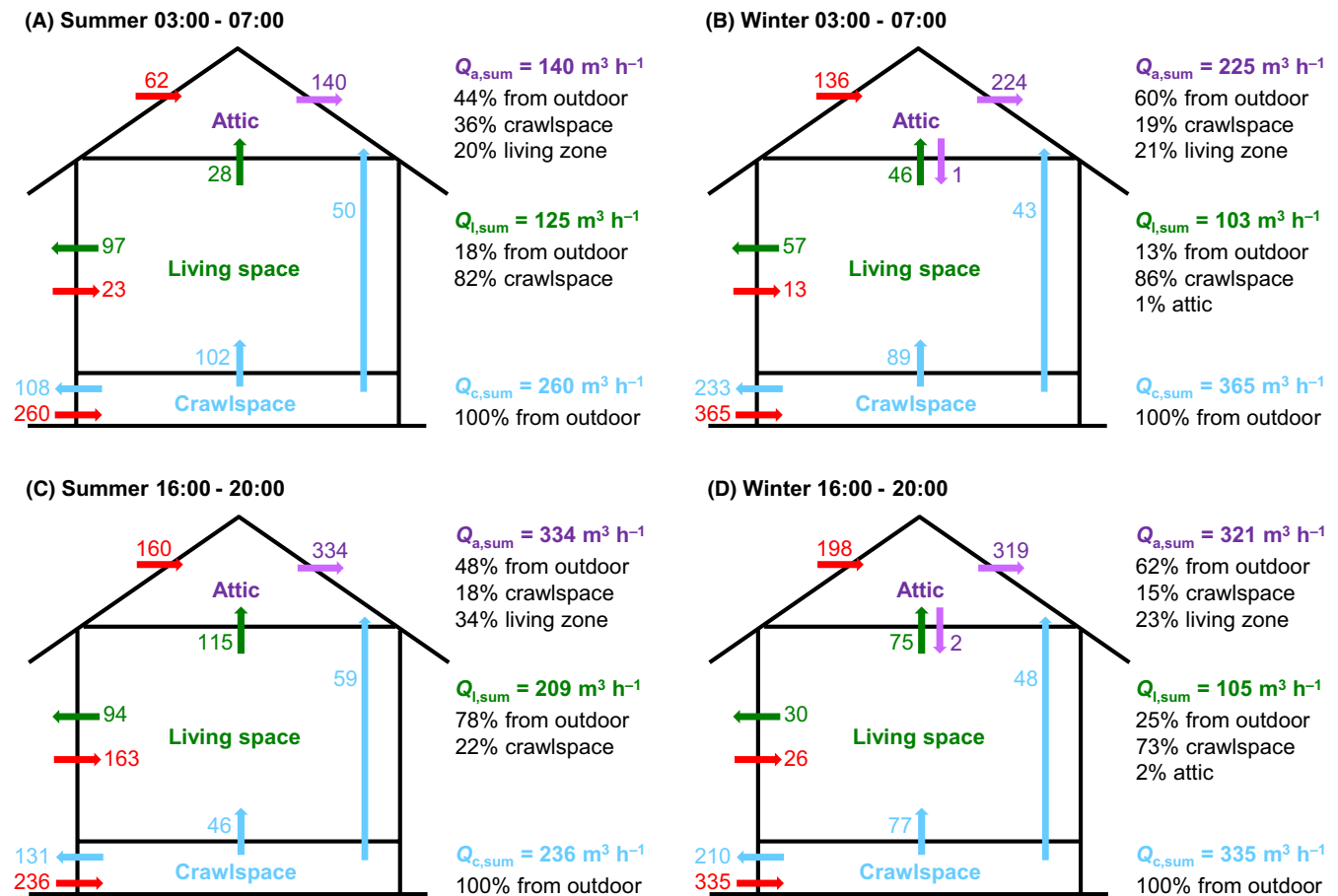


**FIGURE 5** Volumetric airflow rates into and out of the attic, living zone, and crawlspace during occupied periods. Results are presented for (A) summer night (3:00-7:00), (B) winter night (3:00-7:00), (C) summer afternoon (16:00-20:00), and (D) winter afternoon (16:00-20:00). The flow rates were calculated using Equation (4), based on the average of hourly median tracer concentrations in the specific 4-hour period. Arrows colored in red, cyan, green, and purple represent the flows from outdoors, crawlspace, living zone, and attic, respectively. The long cyan arrow represents a direct airflow path from the crawlspace to the attic. The numbers on the arrows represent estimated flow rates in  $\text{m}^3 \cdot \text{h}^{-1}$ . On the right of each panel are reported the total flow rates into the attic, living zone, and crawlspace, along with percentage contributions from each space

Strong wind effect on attic airflows has been reported in an earlier study.<sup>35</sup>

Figure 5 documents important findings about the flow paths for air entering the living zone of the study house. First, for 3 of the 4 periods plotted in Figure 5, more than 70% of the total airflow entering the living zone came through the crawlspace rather than entering directly from outdoors. The exception was summer afternoons, when 78% of the airflow came from outdoors and 22% through the crawlspace. Two coupled features are prominently different for summer afternoons compared with the other periods: small indoor-outdoor temperature difference (hence a small stack effect) and large number of open windows. Another important observation about airflow patterns in this house is the negligible contribution of flow from the attic entering the living zone. Little such flow could even be detected during the summer as the living-space concentration of the tracer gas released in the attic was almost always below the detection limit. In the winter, a modest flow from the attic into the living zone was inferred from the tracer gas results; however, the associated flow rate only represented 1%-2% of the total flow entering the living zone.

Undetectable airflow from attic to the living zone has been reported for 2 research houses previously;<sup>13,14</sup> significant downward airflow from attic to the living zone was measured in other test houses.<sup>15,16</sup> In particular, Fortmann et al<sup>16</sup> reported that the downward airflow from attic to living zone was around 80% of the reverse upward flow in a test house in Maryland, and the corresponding value was 5%-30% for a second house after a house-tightening retrofit procedure.

The substantial upward interzonal airflows with negligible downward airflow in the house studied here are attributable to the stack effect, but with a wrinkle. To promote any sustained downward airflow between the attic and the living zone via the stack effect, air temperature in both the attic and the living zone would need to be lower than the outdoor temperature. Analogous conditions would need to prevail for flow downward from the living zone to the crawlspace. In a few instances when both  $T_{in} - T_{out}$  and  $T_{crawlspace} - T_{out}$  were significantly negative for a few hours, the living zone tracer was indeed clearly detected in the crawlspace (eg Figure S12). These episodes correspond a heat wave passing through the region. Such conditions prevailed only 7% of the monitored time during the

summer campaign and were never observed in the winter. On the contrary, for 86% of the time in the summer and 99% of the time in the winter, temperature conditions prevailed as follows:  $T_{in} - T_{out} > 0$  and  $T_{crawl} - T_{out} > 0$ . This combination favored steady upward airflow from the crawlspace to living zone. Temperature conditions that could promote downward airflows from the attic to the living zone (ie  $T_{in} - T_{out} < 0$  and  $T_{attic} - T_{out} < 0$ ) occurred less than 1% of the time in the summer and were never observed in the winter, whereas the upward-flow-inducing combination of  $T_{in} - T_{out} > 0$  and  $T_{attic} - T_{out} > 0$  held for 88% of the time in the summer and 86% in the winter.

Occupants can influence airflow pattern through the operation of furnace, exhaust fans, and the vented clothes dryer. Operation of exhaust fans in the bathrooms and over the stove might depressurize the living space and promote attic air being transported downward. Such fan effects were observed on occasion in the winter (cf. Figure S13), but rarely in the summer. The seasonal difference of fan effects might explain why the median living zone concentration of attic tracer was above detection limit in the winter. Nevertheless, the overall fan effect is small as compared to the prevailing stack effect. Dryer use and furnace operation did not produce discernible effects on interzonal airflows.

### 3.3 | Mixing between the upper and lower living zones

In using tracer gas measurements to determine airflow rates among zones, we have assumed that each zone could be represented as a single well-mixed volume. That type of assumption is common in studies of indoor environmental quality; however, its validity is not often scrutinized.<sup>4,10,36</sup> In this study, we have explored the extent to which the well-mixed approximation is a valid representation of the living zone of the studied house and its impact on estimated air change rate values using tracer methods. We did so by having a different tracer steadily released in the upper and lower living zones, respectively, for portions of the summer and winter campaigns (Figures S5 and S6). We also separately monitored the tracer concentrations in the upper and lower portions of the living zone.

Figure 6 shows hourly variation of the concentrations of the 2 tracers in the 2 seasons. The degree of agreement in tracer concentrations measured in the kitchen (in orange; lower level) and in the bedroom area (in green; upper level) indicates how well the air is mixed throughout the living zone. A perfectly mixed condition would lead to equal concentrations at the 2 locations for both tracers. As shown in Figure 6, the 2 tracers exhibit different degrees of mixing in detail, but the overall impression is one of fairly good mixing between the 2 zones. For the tracer released on the lower level, the median concentration in the kitchen (lower level) and bedroom area (upper level) agreed to within 20% during entire days. For the tracer released on the upper level, the median concentrations in the 2 locations agreed to within 30% for the winter and for most of the time in the summer, yet differences of ~ 50% were observed during summer nights. The better mixing for the tracer released in the lower level

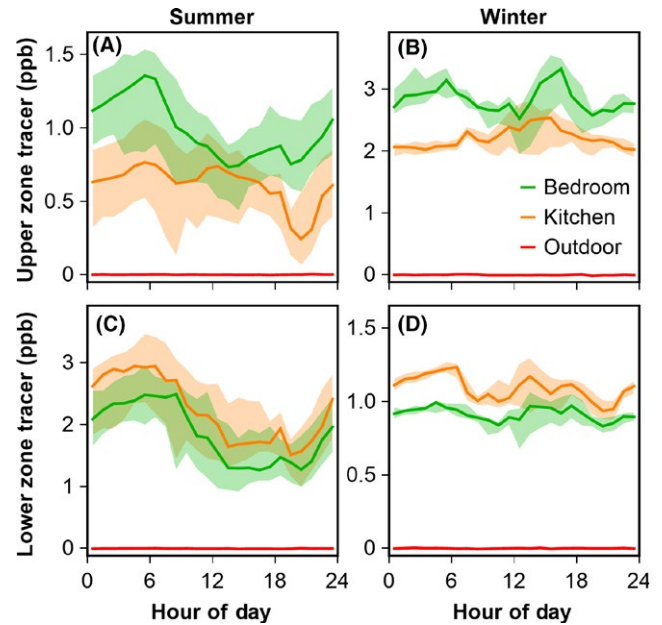


**FIGURE 6** Hourly variation of mixing ratios of tracer compounds injected into the upper (bedroom, top) and lower (kitchen, bottom) levels of the living zone. Data are presented for summer (left) and winter (right), respectively. Data are colored in green, orange, and red for mixing ratios in the bedroom area, kitchen, and outdoors, respectively. The solid line and shaded regions, respectively, represent the median and interquartile ranges of mixing ratios for each hour of the day. The summer data correspond to periods 9, 11, 12, 13, and 15 in Figure S6 and the winter data correspond to period 5 in Figure S7. The 2 tracers injected in the upper and lower levels were reversed in the 2 seasons; consequently, the concentrations are not directly comparable across the seasons

probably relates to the overall upward airflow pattern in the studied house.

The analysis below further evaluates uncertainty or bias in estimated values of air change rate associated with imperfect mixing. Results using 2 categories of methods, with increased complexity, were compared as follows: (1) single-point measurements of a tracer released at a single point; (2) single-point measurements of 2 tracers or measurements of single tracer at 2 locations. Given 2 tracers were released and measurements at 2 points were made, methods (1) and (2) each led to 4 sets of estimates of air change rates. For a perfectly mixed volume, estimated air change rates would not be sensitive to where the tracer was released or where it was measured. The sensitivity of each category of method to the well-mixed assumption is hence discussed in terms of the extent of quantitative agreement among the associated 4 sets of estimates.

Figure 7 plots the 4 sets of estimates of air change rates using the first method against the best estimates reported earlier (based on measurement of 2 tracers at 2 points). Here, the best estimates serve as reference values for comparing different estimates using the first approach; one need not assume that they represent true values. As shown in Figure 7A, the 4 estimates exhibit systematic differences. On average, measurements of the upper living zone tracer in

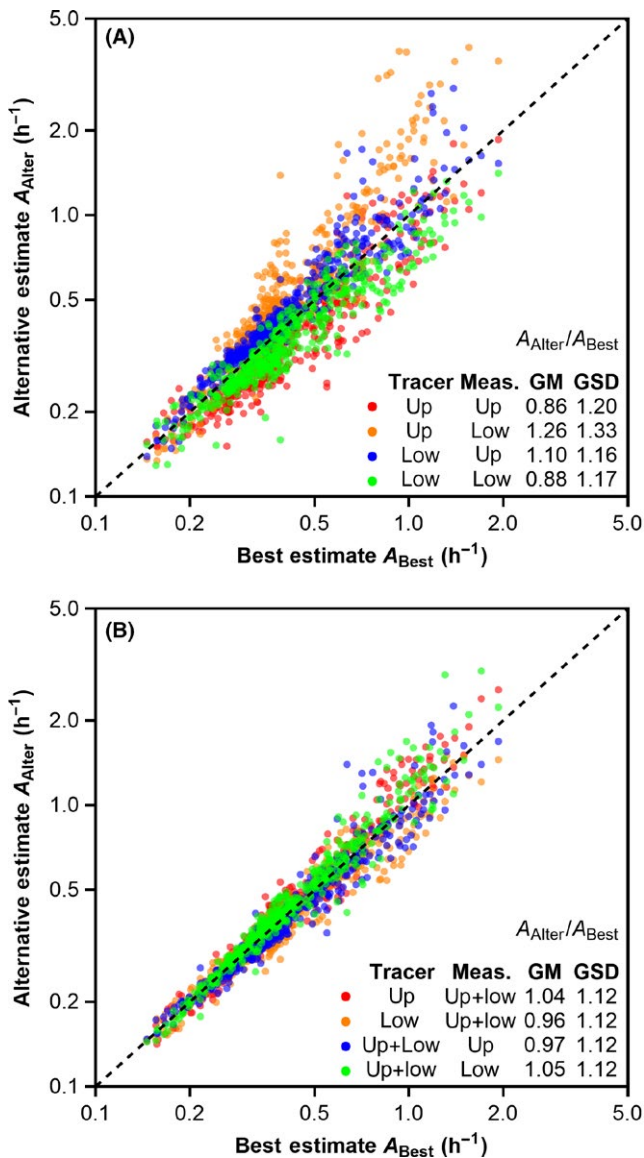


**FIGURE 7** Scatter plot of air change rates estimated using alternative approaches ( $A_{\text{Alter}}$ ) against best estimate air change rate ( $A_{\text{Best}}$ ). Alternative approaches are based on (A) single-point measurements of single tracer and (B) 2-point measurements of single tracer or single-point measurements of 2 tracers. In panel (A), red, orange, blue, green points correspond to estimates using measurement in upper, lower, upper, and lower living zone of tracer released in upper, upper, lower, and lower living zone, respectively. In panel (B), red and orange points correspond to estimates based on 2-point measurements of upper and lower living zone tracer, respectively; blue and green points correspond to estimates based on measurements of 2 tracers in upper and lower living zone, respectively. Geometric mean (GM) and geometric standard deviation (GSD) are listed for the ratio  $A_{\text{Alter}}/A_{\text{Best}}$ . The black dashed line represents a 1:1 line (ie  $A_{\text{Alter}}/A_{\text{Best}} = 1$ )

the lower living zone led to the highest estimates of air change rates (26% higher than the reference level) (Figure 7A), whereas measurements of the upper living zone tracer in the upper living zone led to the lowest estimates (14% lower than the reference level). The estimates using the lower living zone tracer fell in between. The

divergence of the 4 sets of estimates was small for lower air change rates, but it grew as air change rates increased. The conclusion is that even for this fairly well-mixed space, the determined air change rates using the first approach still remains influenced by the location of tracer release and measurement.

Figure 7B plots estimates using the second approach, based on one-point measurements of 2 tracers or 2-point measurements of 1 tracer. All 4 sets of estimates using the second approach agreed well with each other, with differences within 5% (GSD = 1.1) from the best estimates. These results suggest that strategies of either releasing 2 tracers or measuring at 2 locations can effectively reduce bias associated with imperfect mixing.

## 4 | CONCLUSION

Through spatially and temporally resolved measurement of 3 deuterated inert tracers released continuously at constant rates, the current study provides a detailed investigation of air change rates and airflow characteristics in a normally occupied single-family house in northern California during 2 climatic seasons. The results regarding air change rate illustrate how the human occupants, via window-opening decisions and heating system operation decisions, can substantially influence household air change rates. The number of window (and door) openings was found to be the most important first-order predictor of air change rates of the living zone. In winter, by heating the house, occupants also indirectly enhanced the stack effect and led to considerably higher air change rate than occurred during the unheated vacant house-closed condition.

The observed interzonal airflow patterns reveal mechanisms of how coupled hidden spaces, including the crawlspace and attic, affect ventilation of the living zone. Largely associated with the stack effect, there were substantial upward interzonal airflows and yet negligible downward airflows among the living zone, attic, and crawlspace in the studied house. Airflow from the crawlspace accounted for more than 70% of total airflow entering the living zone in the winter and at night in the summer. An implication is that air pollutants emitted in the crawlspace can be carried effectively into the living zone. Such pollutants could include radon emitted from soil or leaked exhaust from a gas burner. As a crawlspace is one of the 3 major substructure types in the United States, airflows from the crawlspace to the living zone and associated pollutant transport merit more attention in future studies. The airflow from the living zone to the attic increased with increasing attic-outdoor temperature differences, suggesting that when the attic is hot, it actively draws air from the living zone, increasing the air change rate of that space. Conversely, negligible airflow occurred from the attic into the living zone. Further studies are warranted for this potentially important effect, which might help to better predict ventilation in many other houses with an attic.

The results also shed light on how air mixing in a split-level living zone can influence the accuracy of air change rates calculated using various tracer methods. Even though tracer data suggest that the

living zone was fairly well mixed, air change rates determined based on one-point measurements of a single tracer can vary considerably with the choice of locations for tracer release and tracer measurement. Either having 2 tracers released at different points or making measurements at 2 different points can effectively reduce the uncertainty associated with imperfect mixing, leading to improved determinations of air change rates. Overall, the results of this study can help to guide future investigations that rely on accurate measurements of airflows and air change rates in single-family residences.

## ACKNOWLEDGEMENTS

This work was funded by the Alfred P. Sloan Foundation via Grant 2016-7050. Y. J. Liu acknowledges support from Alfred P. Sloan Foundation MoBE Postdoctoral Fellowship (Grant 2015-14166). We thank occupants in the studied house for volunteering their house and facilitating and participating in the measurements. We thank Robin Weber for technical assistance. The occupants gave informed consent for this study, which was approved by the Committee for Protection of Human Subjects for the University of California, Berkeley (Protocol #2016-04-8656).

## ORCID

Y. Liu  <http://orcid.org/0000-0001-6659-3660>

P. K. Misztal  <http://orcid.org/0000-0003-1060-1750>

J. Xiong  <http://orcid.org/0000-0001-8057-4263>

Y. Tian  <http://orcid.org/0000-0001-5905-4976>

W. W. Nazaroff  <http://orcid.org/0000-0001-5645-3357>

A. H. Goldstein  <http://orcid.org/0000-0003-4014-4896>

## REFERENCES

- Nazaroff WW, Doyle SM. Radon entry into houses having a crawl space. *Health Phys.* 1985;48:265-281.
- Mills WB, Liu S, Rigby MC, Brenner D. Time-variable simulation of soil vapor intrusion into a building with a combined crawl space and basement. *Environ Sci Technol.* 2007;41:4993-5001.
- Little JC, Daisey JM, Nazaroff WW. Transport of subsurface contaminants into buildings. *Environ Sci Technol.* 1992;26:2058-2066.
- Du L, Batterman S, Godwin C, et al. Air change rates and interzonal flows in residences, and the need for multi-zone models for exposure and health analyses. *Int J Environ Res Public Health.* 2012;9:4639-4661.
- Persily AK. Field measurement of ventilation rates. *Indoor Air.* 2016;26:97-111.
- ASTM International. *ASTM E741-11(2017) Standard Test Method for Determining Air Change in a Single Zone by Means of a Tracer Gas Dilution.* West Conshohocken, PA: ASTM International; 2017.
- Sherman MH, Modera MP. Comparison of measured and predicted infiltration using the LBL infiltration model. In: Trechsel HR, Lagus PL, eds. *ASTM STP 904 Measured Air Leakage of Buildings.* Philadelphia, PA: American Society for Testing and Materials; 1986:325-347.
- Stymne H, Emenius G, Boman CA. Long term ventilation variation in two naturally ventilated Stockholm dwellings. In: *Indoor Air 2005: Proceedings of the 10th International Conference in Indoor Air Quality and Climate*; 2005:3239-3243.
- Wallace LA, Emmerich SJ, Howard-Reed C. Continuous measurements of air change rates in an occupied house for 1 year: the effect of temperature, wind, fans, and windows. *J Expo Anal Environ Epidemiol.* 2002;12:296-306.
- Bekö G, Gustavsen S, Frederiksen M, et al. Diurnal and seasonal variation in air exchange rates and interzonal airflows measured by active and passive tracer gas in homes. *Build Environ.* 2016;104:178-187.
- Persily AK, Axley J. Measuring airflow rates with pulse tracer techniques. In: Sherman MH, ed. *ASTM STP 1067 Air Change Rate and Airtightness in Buildings.* Philadelphia, PA: American Society for Testing and Materials; 1990:31-52.
- Sherman M. A multitracer system for multizone ventilation measurement. *Rev Sci Instrum.* 1990;61:2457-2461.
- Saunders CH. Air movement in houses: a new approach. *Batim Int Build Res Pract.* 1982;10:160-175.
- l'Anson SJ, Irwin C, Howarth AT. Air flow measurement using three tracer gases. *Build Environ.* 1982;17:245-252.
- Dietz RN, Goodrich RW, Cote EA, Wieser RF. Detailed description and performance of a passive perfluorocarbon tracer system for building ventilation and air exchange measurements. In: Trechsel HR, Lagus PL, eds. *ASTM STP 904 Measured Air Leakage of Buildings.* Philadelphia, PA: American Society for Testing and Materials; 1986:203-264.
- Fortmann RC, Nagda NL, Rector HE. Comparison of methods for the measurement of air change rates and interzonal airflows in two test residences. In: Sherman MH, ed. *ASTM STP 1067 Air Change Rate and Airtightness in Buildings.* Philadelphia, PA: American Society for Testing and Materials; 1990:104-118.
- Blomsterberg Å, Carlsson T, Svensson C, Kronvall J. Air flows in dwellings—simulations and measurements. *Energy Build.* 1999;30:87-95.
- Plathner P, Woloszyn M. Interzonal air and moisture transport in a test house: experiment and modelling. *Build Environ.* 2002;37:189-199.
- Rudd AF, Lstiburek JW. Measurement of ventilation and interzonal distribution in single-family homes. *ASHRAE Trans.* 2000;106:709-718.
- Du L, Batterman S, Godwin C, Rowe Z, Chin JY. Air exchange rates and migration of VOCs in basements and residences. *Indoor Air.* 2015;25:598-609.
- Batterman S, Jia C, Hatzivasilis G. Migration of volatile organic compounds from attached garages to residences: a major exposure source. *Environ Res.* 2007;104:224-240.
- Dodson RE, Levy JI, Shine JP, Spengler JD, Bennett DH. Multi-zonal air flow rates in residences in Boston, Massachusetts. *Atmos Environ.* 2007;41:3722-3727.
- Tian Y, Liu Y, Misztal PK, et al. Fluorescent biological aerosol particles: concentrations, emissions, and exposures in a northern California residence. *Indoor Air.* 2018; <https://doi.org/10.1111/ina.12461>.
- Atkinson R, Baulch DL, Cox RA, et al. Evaluated kinetic and photochemical data for atmospheric chemistry: volume II — gas phase reactions of organic species. *Atmos Chem Phys.* 2006;6:3625-4055.
- Sinden FW. Multi-chamber theory of air infiltration. *Build Environ.* 1978;13:21-28.
- Sandberg M. The multi-chamber theory reconsidered from the viewpoint of air quality studies. *Build Environ.* 1984;19:221-233.
- Sherman MH. On the estimation of multizone ventilation rates from tracer gas measurements. *Build Environ.* 1989;24:355-362.
- Sandberg M, Stymne H. The constant tracer flow technique. *Build Environ.* 1989;24:209-219.

29. Nazaroff WW, Feustel H, Nero AV, et al. Radon transport into a detached one-story house with a basement. *Atmos Environ.* 1985;19:31-46.
30. ASHRAE. Standard 62.2 Ventilation and Acceptable Indoor Air Quality in Low-Rise Residential Buildings; 2010.
31. Nabinger S, Persily A. Impacts of airtightening retrofits on ventilation rates and energy consumption in a manufactured home. *Energy Build.* 2011;43:3059-3067.
32. Malik N. Field studies of dependence of air infiltration on outside temperature and wind. *Energy Build.* 1978;1:281-292.
33. Breen MS, Breen M, Williams RW, Schultz BD. Predicting residential air exchange rates from questionnaires and meteorology: model evaluation in central North Carolina. *Environ Sci Technol.* 2010;44:9349-9356.
34. Howard-Reed C, Wallace LA, Ott WR. The effect of opening windows on air change rates in two homes. *J Air Waste Manage Assoc.* 2002;52:147-159.
35. Walker IS, Forest TW. Field measurements of ventilation rates in attics. *Build Environ.* 1995;30:333-347.
36. Van Ryswyk K, Wallace L, Fugler D, et al. Estimation of bias with the single-zone assumption in measurement of residential air exchange using the perfluorocarbon tracer gas method. *Indoor Air.* 2015;25:610-619.

#### SUPPORTING INFORMATION

Additional supplemental material may be found online in the Supporting Information section at the end of the article.

**How to cite this article:** Liu Y, Misztal PK, Xiong J, et al. Detailed investigation of ventilation rates and airflow patterns in a northern California residence. *Indoor Air.* 2018;00:1-13. <https://doi.org/10.1111/ina.12462>